

SUPPLEMENTAL INFORMATION ON THE ROLE OF DISSOLVED SILICA ON THE BIODEGRADATION OF OCTYLAMINE

Hildegard Selig, Kim F. Hayes* and Peter Adriaens

Mineralization kinetics of octylamine in the presence and absence of silica: modeling methods.

The Haldane modification of the Monod equation was adopted to describe the inhibitory effect of octylamine on biodegradation rates, which expressed in terms of substrate utilization, has the differential form:

$$-\frac{dS}{dt} = \frac{\mu_{\max} S}{K_s + S + S^2/K_i} \left(S_o + \frac{X_o}{Y} - S \right) \quad (1)$$

where μ_{\max} is defined as the maximum specific growth rate (1/hr), K_s as the Monod affinity constant (mg/L), and K_i as Haldane inhibition constant (mg/L). Equation 1 is combined with the following equation to account for the ^{14}C concentration present in solution in compounds or phases different from the parent compound, octylamine:

$$^{14}\text{C} = \zeta S_o + (1 - \zeta) S \quad (2)$$

Non-linear regression techniques present problems inherent to any iterative process, such as selection of initial values, lack of convergence and the estimation of reliable confidence intervals. In addition, the limited amount of biodegradation data collected (usually only duplicates or triplicate samples are generated) compromise the reliability of most of the techniques based on classical statistics. In this study, a random

data simulator was used to generate data within the experimental error to allow parameter estimation from a limited set of experimental data. The non-linear regression problem in substrate utilization kinetics was approached from an optimization point of view, since what is needed is a set of parameter values that minimizes the difference between observed (S) and calculated (\hat{S}) substrate concentrations expressed as an objective function. The weighted sum-of-the square differences was selected as the objective function,

$$\min R = \sum w_i (S_i - \hat{S}_i)^2 \quad (3)$$

in which the weight, w_i , is determined by the functional form of the data. In this study, w_i was assigned to be the inverse of the substrate concentration ($1/S_i^2$).

In this study, global minimization of the residuals was obtained by using as initial parameter values the values calculated using multiple linear regression models. The Haldane equation expressed in terms of the specific rate of substrate utilization ($q_r = Y/X \, dS/dt$) can be written as:

$$q_r S = \mu_{\max} S - \frac{1}{K_i} q_r S^2 - K_s q_r \quad (4)$$

after multiplying each term by $(K_s + S + S^2/K_i)$, and simplifying terms. Equation 4 is a linear expression of the form

$$y = k_1 f_1(S) + k_2 f_2(S) + k_3 f_3(S) \quad (5)$$

where

$$k_1 = \mu_{\max}, \quad k_2 = -1/K_i, \quad k_3 = -K_s, \quad f_1(S) = S, \\ f_2(S) = q_r S^2, \quad f_3(S) = q_r \quad \text{and} \quad y = q_r S$$

and amenable for multiple regression analyses to determine μ_{\max} , K_s and K_i .

Initial cell densities (the concentration of cells at the onset of steady-state conditions or detectable substrate consumption) were determined independently from the kinetic parameter evaluation with the aid of error analyses based on the log-growth equation expressed in terms of cell mass or substrate utilization.

A method based on Montecarlo simulation techniques was used to obtain reliable average parameter values and their confidence intervals. In this method, large sets of randomly generated data are obtained within the experimental error. Non-linear techniques are applied to each set of simulated data, and large sets of kinetic parameters are obtained. The confidence intervals and the average values of each parameter are subsequently estimated from the frequency distribution of the parameter.

Kinetic parameters μ_{\max} , K_s and K_i and the fraction ζ were estimated by applying a non-linear regression routine to 50 sets of data randomly generated (Microsoft Excel 5.0) within the experimental observation values. For sample duplicates a and b at any time t, the simulated i term can be expressed as:

$$S_i = \left(\frac{S_a + S_b}{2} \right) + |S_a - S_b| \text{rdn}_i \quad (6)$$

where rdn_i represents the random number corresponding to the i term.

Using equation 6, fifty sets of simulated data were obtained resulting in fifty estimates for each kinetic parameter. The 95% confidence intervals were then calculated from the frequency distribution of each parameter by computing the limits of the interval at the 2.5% and 97.5% probability of occurrence from each distribution. The reported average value for each parameter is the mean of the parameter values comprised in the 95% confidence interval. Finally, sensitivity analyses were performed, in which the initial parameter values were varied widely to test the uniqueness of the solution.

A step by step chronology of the activities involved in kinetic modeling approach used is presented in Figure SI-1. These activities are as follows: i) the calculation of initial cell densities, ii) the calculation of the initial parameter values, iii) the generation of simulated data, iv) the application of non-linear regression techniques for parameter estimation, v) the calculation of confidence intervals, and vi) the determination of the stability of the parameter values.

Uniqueness of the solution

The values of the objective function are presented in three-dimensional contour plots for both silica-free (Figure SI-2) and silica-containing systems (Figure SI-3). The parameter μ_{\max} was varied within 10% of the optimal value at 0.01 intervals while K_s was varied from 1.25 to 0.25 times the optimal value at 0.05 intervals. K_i was held constant for the contour plots. For both systems, a unique minimum for the objective function exists as shown by the closed contour line around the minimum. Open contour lines, however, were found for μ_{\max}/K_i or K_s/K_i variations, suggesting multiple pairs of

estimated values in the 10% sub-optimal range. However, the lack of sensitivity of the K_i term in equation 2 at high values of K_i , appears to be the culprit of the apparent problem. Figure SI-4 shows the values of the objective function at different values of K_i at the optimal point. At low K_i values, the objective function sharply approaches its minimum, while not so dramatic variations are shown at larger values of K_i . Nevertheless, the minimum value of the objective function corresponds to the solution value of K_i given in Table 5 in the manuscript

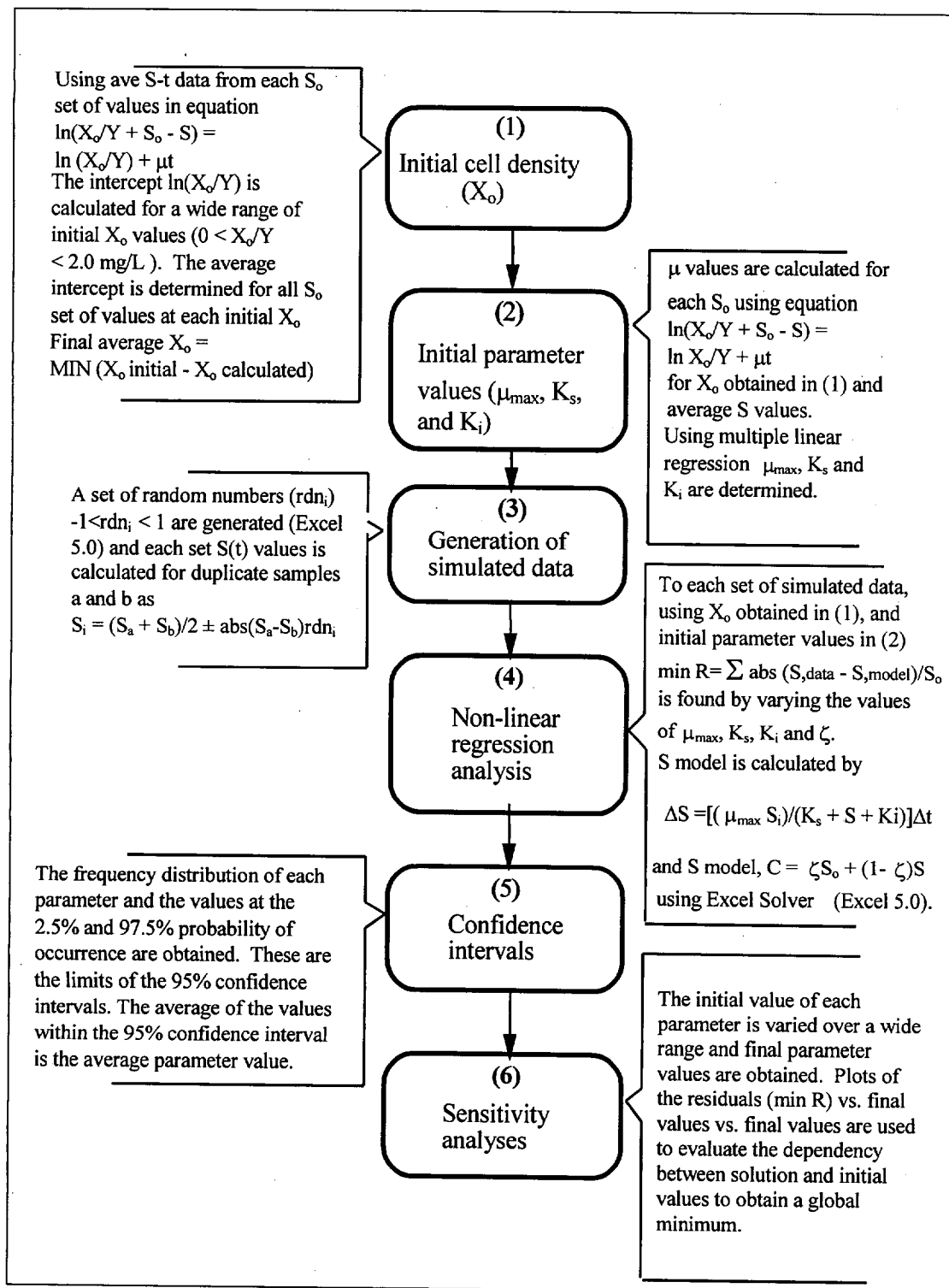


Figure SI-1. Sequential diagram of activities involved in parameter estimation in the kinetic study of octylamine mineralization.

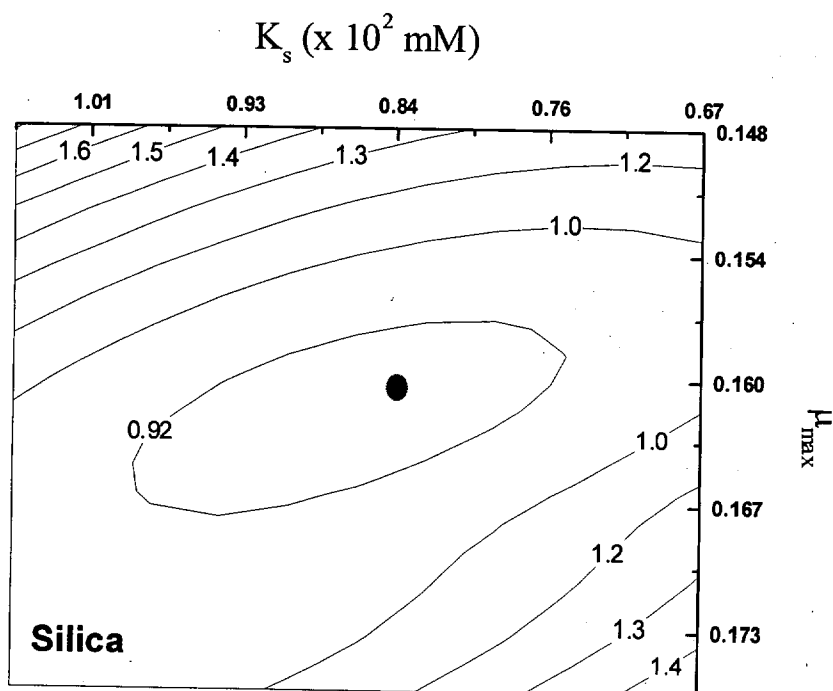


Figure SI-2. Objective function dependency at variations of K_s and μ_{max} for the silica-containing system. The dark circle represents the global minimum.

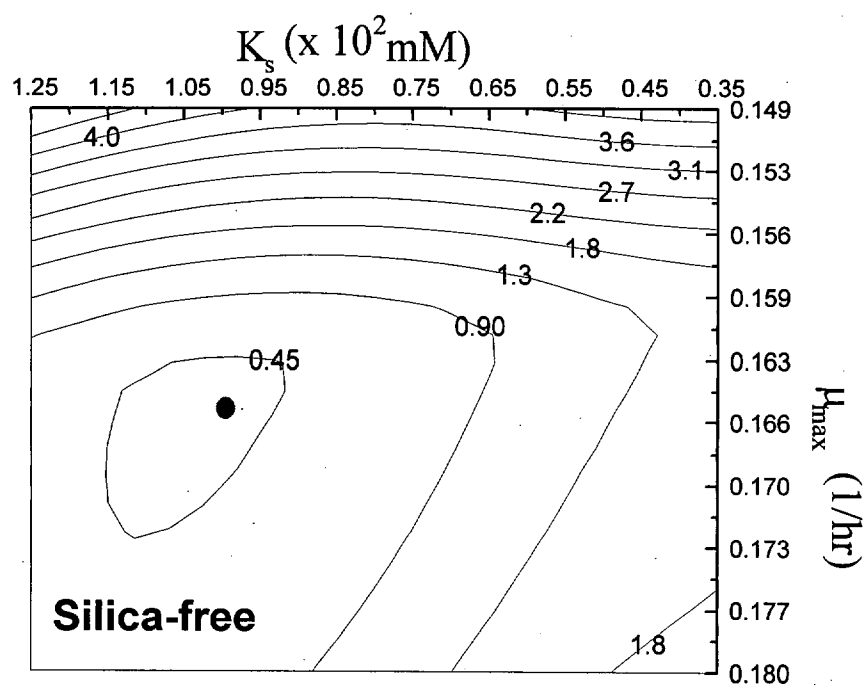


Figure SI-3. Objective function dependency at variations of K_s and μ_{\max} for the silica-free system. The dark circle represents the global minimum.

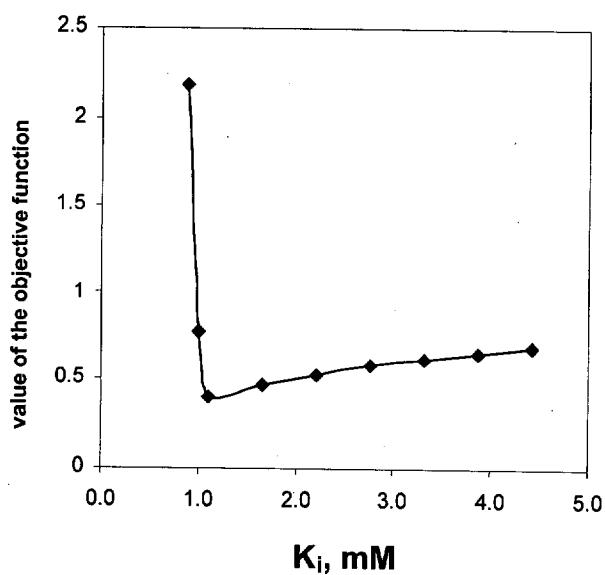


Figure SI-4. Variations of K_i with respect to the objective function values.

Captions

Figure SI-1. Sequential diagram of activities involved in parameter estimation in the kinetic study of octylamine mineralization.

Figure SI-2. Objective function dependency at variations of K_s and μ_{\max} for the silica-containing system. The dark circle represents the global minimum.

Figure SI-3. Objective function dependency at variations of K_s and μ_{\max} for the silica-free system. The dark circle represents the global minimum.

Figure SI-4. Variations of K_i with respect to the objective function values.